Macromolecules
ARTICLE

Macromolecules **2010**, *43*, 10055–10063 **10055**
DOI: 10.1021/ma1017378

Abrupt Shear Thickening of Aqueous Solutions of Hydrophobically Modified Poly(*N*,*N*′-dimethylacrylamide-*co*-acrylic acid)

Ashish Lele,[†] Aarti Shedge,[†] Manohar Badiger,*[,†] Prakash Wadgaonkar,[†] and Christophe Chassenieux[‡]

[†]*Polymer Science and Engineering Division, National Chemical Laboratory, Pune 411 008, India, and* [‡]*Polymer, Colliods and Interfaces UMR CNRS 6120, Universite du Maine, Avenue Olivier Messiaen 72085, Le Mans, cedex 09, France*

Received July 30, 2010; Revised Manuscript Received October 17, 2010

ABSTRACT: We report some new and interesting observations on the abrupt and large shear-induced thickening of aqueous solutions of hydrophobically modified poly(*N*,*N*′-dimethylacrylamide-*co*-acrylic acid). High molecular weight copolymer was prepared by free radical copolymerization of *N*,*N*′-dimethylacrylamide [DMA] and acrylic acid [AA] and was subsequently modified to different extents using a hydrophobic compound, namely, 3-pentadecylcyclohexylamine [3-PDCA], which is derived from a renewable resource material, cashew nutshell liquid [CNSL]. The structural elucidation of the base copolymer and the hydrophobically modified copolymers was performed by ^{1}H and ^{13}C NMR spectroscopy. The zero shear viscosities [η_0] of the hydrophobically modified polymers were lower than that of the precursor poly(*N*,*N*′-dimethylacrylamide-*co*-acrylic acid) until some critical polymer concentration, which increased with increase in hydrophobic modification. Above the critical concentrations, the η_0 of the hydrophobically modified copolymers surpassed that of the precursor at the same concentration. At moderate shear rates some of these hydrophobically modified copolymers exhibited an abrupt shear-induced thickening in which the viscosity of the samples increased severalfold. We show here from creep experiments that thickening occurs only when the shear rate reaches a critical value, $\dot{\gamma}_{crit}$, and that the thickened samples can be trapped in different metastable states by controlling the applied stress. Interestingly, the shear thickened samples showed further thickening upon decreasing the applied stress. Eventually, the metastable samples revert to their equilibrium states at characteristic time that depends on (small) probe stress.

1. Introduction

In general, most polymer melts and solutions display shear thinning behavior. The opposite behavior of an increase in viscosity with an increase in shear, i.e. shear thickening, is less commonly encountered. The phenomenon of shear thickening is often observed in physically cross-linked networks of polymer chains having a few localized, energetically favored interactions such as in ionomers[1] and aqueous solutions of hydrophobically modified polymers.[2,3] Shear thickening polymers are industrially important as viscosity modifiers for polymer augmented water flooding in enhanced oil recovery (EOR). Shear thickening has also been observed in wormlike micellar solutions[4] and concentrated suspensions.[5]

Several theoretical models have been proposed to explain the viscoelastic behavior of associating polymer solutions. The mathematical framework for these models was first provided by Tanaka and Edwards (TE),[6−9] who developed a transient network theory based on the affine network model of Green and Tobolsky.[10] In the TE model for telechelic associating polymers containing two hydrophobic "sticker" groups at chain ends, the cross-links under quiescent conditions have a finite lifetime, which decreases with imposed shear deformation. Consequently, the model predicts shear thinning but fails to describe the shear thickening property of associating polymer solutions. The molecular cause of shear thickening phenomenon in polymer solutions was suggested to be shear-induced transfer of intramolecular interactions to intermolecular interactions.[11,12] Wang[13] argued that free polymer chains, under the action of shear, can join the transient network first as dangling chains and eventually as bridging chains which are elastically active. This model predicted shear thickening albeit at shear rates much higher than the experimentally observed range. Marucci et al.[14] suggested that a bridging chain would pull out of its associations only when shear is able to stretch it to nearly its full extent such that the accompanying non-Gaussian chain stretching might cause shear thickening before thinning occurs. Similar observations were also made by others.[15] However, the predicted extent of thickening was much smaller than experimental observations. In the same paper the authors also suggested an alternative mechanism in which bridging chains relax only partially upon breakage of associations since they are likely to be trapped into other associations before complete relaxation. Brownian dynamic simulations[16] supported this idea and suggested that the rate of associations in fact depends on the chain extension. Subsequently, Vaccaro and Marucci[17] revised the earlier model and were able to predict shear thickening at intermediate shear rates in qualitative agreement with experiments. Ahn and Osaki[18] proposed alternative kinetics for the rates of network creation and destruction. Lele and Mashelkar[19] used this model to predict anomalous gelation effects in transient networks. Further refinements of the network model by Tripathi et al.[20] allowed nearly quantitative model fits to experimental shear thickening data in both shear and extension. Some researchers have also explained the mechanism of shear thickening on the basis of association of aggregates containing many chains under shear.[21,22]

The above theoretical models predict a gradual shear thickening with increase in shear rate followed by shear thinning, in

*Corresponding author. E-mail: mv.badiger@ncl.res.in.

Published on Web 11/08/2010

agreement with most experimental observations. However, Bokias et al.[23] recently reported on the shear rheology of a copolymer of poly(*N*-isopropylacrylamide-*co*-*N*,*N*′-[(dimethylamino)propyl]-methacrylamide) of high molecular weight and demonstrated an *abrupt* shear thickening effect of *large magnitude* at a critical shear rate, $\dot{\gamma}_{crit}$, which decreased with increasing polymer concentration and decreasing temperature. Subsequently, Cadix et al.[24] investigated the rheology of high molecular weight poly(*N*,*N*′-dimethylacrylamide-*co*-acrylic acid) which was hydrophobically modified using linear alkylamines. In the linear viscoelastic regime the copolymer showed scaling laws that were in apparent agreement with the so-called "sticky reptation" model[25] where as at high shear rates abrupt shear-induced thickening was observed at critical shear rates which decreased with polymer concentration as $\dot{\gamma}_{crit} \sim C_p^{-3}$ and also with increasing hydrophobic content. More recently, Wang et al.[26] investigated the nonlinear rheological properties of the same solutions in a dynamic mode and concluded that shear thickening is caused by an increase in the lifetime of associations.

On the basis of the observations made from earlier reports, it appears that the prerequisites for associating polymers to exhibit an abrupt shear thickening effect in experimentally observable range of shear rates are (i) the polymer should possess an appropriate balance of hydrophobic and hydrophilic interactions such that in a solution it is on the threshold of phase separation yet shows complete solubility and (ii) the concentration of the polymer should be close to a critical aggregation concentration, C_{agg}. Furthermore, the nature of the hydrophobic compound, the charges on the polymer chain, the molecular weight of the polymer, and the presence of salt and surfactants largely influence the shear thickening behavior. Despite a few interesting studies on such polymer solutions, the abrupt shear-thickening phenomenon remains largely not understood. None of the transient network models for associating polymers mentioned above can predict an abrupt shear thickening effect in associating polymers.

In most previous rheological studies on associating polymer solutions, the shear thickening effect has been investigated using a strain-controlled rheometer in a rate-ramp mode. The intrinsic difficulty with this experiment, especially in the case of solutions that show abrupt thickening, is that the large imposed strain tends to rupture the thickened samples or eject it out of the geometry. On the other hand, if similar experiments were to be done in a stress-ramp mode, the rate of deformation tends to decrease as the sample thickens, thereby minimizing the chances of damage to the sample. In this work we have used creep experiments to demonstrate several interesting features of the abrupt shear thickening phenomenon in hydrophobically modified polymer solutions. In particular, we will show that creep experiments provide a facile control on trapping the thickened sample in different metastable states. Our results also show that upon reduction of the imposed stress the thickened sample undergoes an *increase* in stiffness. Eventually at low stress, the thickened sample relaxes to its equilibrium state after a critical liquefaction time and at a critical strain.

For our studies we have used a high molecular weight poly(*N*,*N*′-dimethylacrylamide-*co*-acrylic acid) copolymer which is modified with a hydrophobic compound, 3-pentadecylcyclohexylamine [3-PDCA]. This particular hydrophobe contains a $-C_{15}H_{31}$ side chain attached to an aliphatic six-membered ring[27] and is prepared from a renewable resource material namely, cashew nutshell liquid (CNSL). According to some literature reports,[28] aliphatic ring compounds are more hydrophobic as compared to linear and aromatic hydrophobic compounds with a similar number of carbon atoms. Therefore, we presume that a small amount of 3-PDCA is sufficient to provide the requisite hydrophobicity for observing shear thickening behavior in our copolymers. The backbone copolymer poly(*N*,*N*′-dimethylacrylamide-*co*-acrylic acid) is similar to that used in earlier studies,[25,26] and it is easy to synthesize with high molecular weights. Further, it allows for tunable hydrophilic−hydrophobic properties and exhibit limited solubility in water, which seems to be a prerequisite for the occurrence of abrupt shear thickening.

2. Experimental Section

2.1. Materials. *N*,*N*′-Dimethylacrylamide (DMA), acrylic acid (AA), 3-pentadecylphenol, sodium metabisulfite ($Na_2S_2O_5$), and ammonium per sulfate [$(NH_4)_2S_2O_8$] were purchased from Aldrich Chemicals. Dicyclohexylcarbodiimide (DCC), *N*-methyl-2-pyrrolidone (NMP), dichloromethane, and diethyl ether were purchased from Merck, India. All the chemicals were of synthesis grade and used as received. The polymer samples were prepared in DI water (18 Ω) with a required concentration.

2.2. Synthesis. *2.2.1. Preparation of the Hydrophobic Compound, 3-Pentadecylcyclohexylamine (3-PDCA).* 3-PDCA was synthesized starting from 3-PDP in four steps: (i) reduction of 3-PDP to 3-pentadecylcyclohexanol; (ii) oxidation of 3-pentadecylcyclohexanol to 3-pentadecylcyclohexanone; (iii) conversion of 3-pentadecylcyclohexanone to 3-pentadecylcyclohexanoneoxime; (iv) reduction of 3-pentadecylcyclohexanone oxime to 3-pentadecylcyclohexylamine. The detailed synthesis procedure is reported earlier.[27] The new hydrophobic compound 3-PDCA is a solid with off-white color. It is soluble in chloroform, dichloromethane, 1-methyl-2-pyrrolidone, diethyl ether, and 1, 4-dioxane and insoluble in methanol and ethanol.

2.2.2. Preparation of Copolymer of Poly(N,N′-dimethylacrylamide-co-acrylic acid) and Its Hydrophobic Modification Using 3-PDCA. The synthesis of polymer involves two steps: In the first step, precursor copolymer of poly(*N*,*N*′-dimethylacrylamide-*co*-acrylic acid) was prepared, and in the second step, some of the acrylic acid units in the copolymer were modified using 3-PDCA. The detailed procedure for the synthesis of precursor polymer and its subsequent hydrophobic modification is reported below.

a. Synthesis of Precursor, Poly(N,N′-dimethylacrylamide-co-acrylic acid) [(70 mol % DMA/30 mol % AA)]. Into a 500 mL three-necked jar reactor, 26 g (0.264 mol) of *N*,*N*′-dimethylacrylamide (DMA) and 8.1 g (0.112 mol) of acrylic acid (AA) were added in 220 mL of water. The pH was adjusted between 8 and 10 by adding 20 mL of 1 M NaOH. The homogeneous mixture obtained by stirring was deaerated with argon gas for 30 min. 0.72 g (0.0031 mol) of ammonium persulfate and 18 mg (0.095 mol) of sodium metabisulfite were added. The polymerization was allowed to proceed for 90 min at 30 °C. The reaction was quenched by adding 10 mL of 3 M HCl, and the polymer was dialyzed against pure water for 1 week and finally recovered by freeze-drying. The yield of the copolymer was found to be 70%. The content of AA incorporated in the copolymer was estimated by ^{13}C NMR spectroscopy.

b. Hydrophobic Modification of Poly(N,N′-dimethylacrylamide-co-acrylic acid) Using 3-PDCA. Into a 500 mL two-neck round-bottom flask, 6 g of precursor polymer was dissolved in 200 mL of *N*-methyl-2-pyrrolidone (NMP) at 70 °C for 12 h. To this solution 0.59 g (0.0019 mol) of 3-PDCA (dissolved in 10 mL of NMP) and 1.98 g (0.0096 mol) of DCC (dissolved in 10 mL of NMP) were added, and the reaction was continued at 70 °C for 12 h. The reaction pathway for the hydrophobic modification is shown in Scheme 1. Then the reaction mixture was allowed to cool to room temperature and precipitated in 3 L of diethyl ether. The precipitated polymer was filtered and dried under vacuum at 50 °C. In order to purify the polymer, the dry polymer was again dissolved in 300 mL of chloroform and precipitated in 3 L of diethyl ether. This process was repeated to get pure polymer, which was dried at 50 °C under vacuum. The dry polymer was then dissolved in deionized water, and the carboxylic groups in the polymer were neutralized with 1 M NaOH. This solution was dialyzed against water and recovered by freeze-drying. Using the above procedure, polymers with different hydrophobic content

Scheme 1. Reaction Scheme for the Preparation of the Hydrophobically Modified Poly(*N*,*N*′-dimethylacrylamide-*co*-acrylic acid)

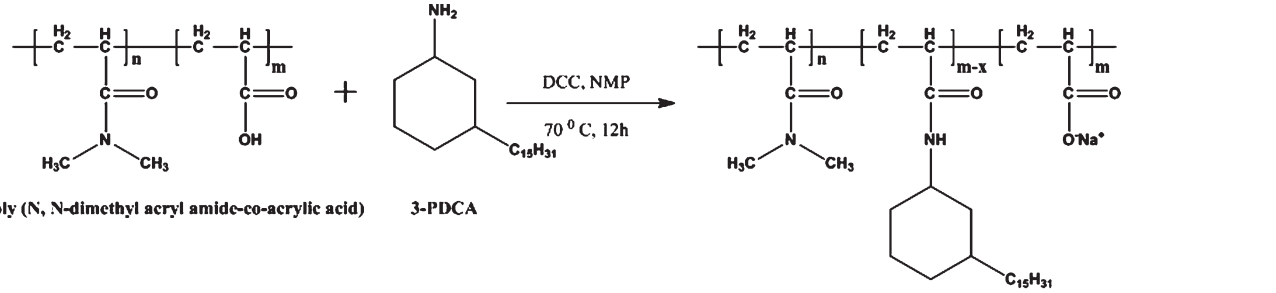

Table 1. Stoichiometry for the Hydrophobic Modification of Poly(*N*,*N*′-dimethylacrylamide-*co*-acrylic acid)

polymer	polymer (g)	3-PDCA (mol %)	3-PDCA (g)	DCC (g)
70DMA/29AA/3-PDCA-1	4	1	0.135	0.45
70DMA/28AA/3-PDCA-2	4	2	0.271	0.904
70DMA/27AA/3-PDCA-3	4	3	0.407	1.36

Table 2. Fraction of Elastically Active Chains in Shear-Induced Gels

stress (Pa)	J_0 (1/Pa)	ν/ν_{max}
8	12 500	3×10^{-8}
10	8110	5×10^{-8}
15	3410	1×10^{-7}
25	585	7×10^{-7}
a	~0.3	1×10^{-3}

[a] Any value $\sigma < \sigma_{crit}$ after gelation.

(1−3 mol %) were prepared. Beyond 3 mol % of 3-PDCA content, the polymer was insoluble in water, and therefore, the hydrophobic content was restricted to 3 mol %. The stoichiometry of reagents used in the reactions is reported in Table 1.

The nomenclature of the polymer prepared is described in Table 1. For example, 70DMA/29AA/3-PDCA-1 corresponds to a copolymer consisting of 70 mol % of DMA, 29 mol % of AA, and 1 mol % of 3-PDCA.

2.3. Characterization. *2.3.1. Gel Permeation Chromatography*. Molecular weight of precursor polymer was determined using 0.1 M $NaNO_3$ as a mobile phase and pectin as standards. 10 mg of polymer was dissolved in 10 mL of 0.1 M $NaNO_3$, and solution was filtered through a 0.45 μm filter (Table 2) [instrument: simple and double detection RD-UV, GPC column: HF-PW-5000 (60 cm)].

2.3.2. Nuclear Magnetic Resonance Spectroscopy. The structural characterization and the composition of the precursor copolymer were determined by ^{13}C NMR spectroscopy which was recorded in DMSO-d_6 using a Bruker DRX-500 spectrometer operating at a ^1H frequency of 500 MHz. For hydrophobically modified polymers, structural characterization was done by ^1H NMR spectroscopy. ^1H NMR spectra were recorded in DMSO-d_6 using a Bruker AV-400 spectrometer operating at a ^1H frequency of 400 MHz.

The precursor and hydrophobically modified samples were dissolved in DMSO-d_6, and ^1H NMR spectra were recorded. All samples were allowed to dissolve for 4−5 days for homogenization before recording the spectra (polymer concentrations for ^1H NMR and ^{13}C NMR were 20 mg/0.7 mL and 100 mg/0.9 mL, respectively).

2.3.3. Sample Preparation. Polymer solutions of desired concentrations (C_p; g/L) were prepared by dissolving a known amount of polymer in water with gentle stirring. The solutions were homogenized for at least 7 days before use. Samples were designated as follows: 70DMA/27AA/3-PDCA-3 implies a hydrophobically modified poly(*N*,*N*′-dimethylacrylamide-*co*-acrylic acid) containing 70 mol % DMA, 27 mol % AA, and 3 mol % of 3-PDCA. The polymer concentration for each solution is specified separately.

2.3.4. Rheology. Rheological properties of the copolymer solutions were studied using two rotational rheometers: a stress-controlled rheometer MCR-301 (Anton Paar) and a strain-controlled rheometer ARES (Rheometric Scientific). Isothermal steady shear experiments were performed in a rate-ramp mode on the ARES and in a stress-ramp mode on the MCR-301. A majority of the rheological studies performed in this work were based on isothermal creep experiments, which were carried out on the MCR-301. Compliance data obtained using small values of the applied stress were used to determine the zero-shear viscosity (η_0). Concentric cylinder geometries and Peltier heating systems were used in all experiments in both rheometers.

3. Results

3.1. Molecular Characteristics of the Precursor Polymer. We have chosen the molar ratios of DMA:AA as 70:30 in order to have reasonably good solubility of the copolymer in water even after hydrophobic modification of the acrylic acid up to 3 mol %. We observed that if the AA content was chosen to be less than 30 mol %, then the hydrophobically modified polymer became insoluble at 3 mol % content of 3-PDCA.

We show in Figure 1 the ^{13}C NMR spectrum of poly(DMA-*co*-AA) [70:30] recorded in DMSO-d_6. The carbonyl (⟩C═O) peak coming from the amide group of DMA appears at 177 ppm, and the carbonyl (⟩C═O) peak coming from acid group of AA appears at 174 ppm. This difference in the chemical shifts of the carbonyl carbons was used to determine the composition of the copolymer. Accordingly, the integration of carbonyl signal of amide and acid gave the ratio of DMA:AA as 70:28. This clearly indicates that the reaction goes toward completion with 98% incorporation of AA units. The other carbon atoms of the main chain and side chain appear in the range 35−40 ppm.

Although the reactivity ratios of DMA and AA are not known, an analogy can be made with the pair of acrylamide/acrylic acid due to similarity in the chemical structures of acrylamide and *N*,*N*′-dimethylacrylamide. The reactivity ratios of acrylamide and acrylic acid in basic pH are known to be respectively $r_1 = 1.32$ and $r_2 = 0.35$. As a consequence, one can expect blocks of DMA to form more favorably in the copolymer rather than a random structure. However, the sequence lengths of DMA and AA units in the copolymers were not analyzed in this work.

The weight-average molecular weight of the copolymer as determined by GPC was found to be $M_w = 1254$ kg/mol (pectin standards) with a PDI of 2.7.

3.2. Hydrophobic Modification of the Precursor Polymer. The incorporation of 3-PDCA on the precursor polymer backbone was confirmed from ^1H NMR spectroscopy.

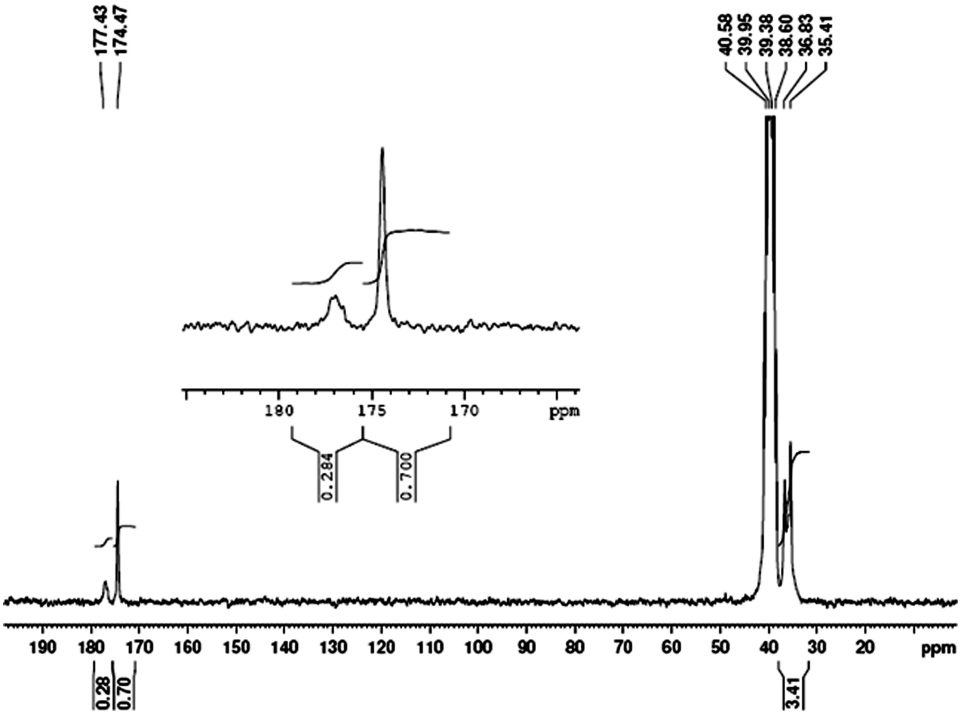

Figure 1. ^{13}C NMR spectrum of poly(*N*,*N*′-dimethylacrylamide-*co*-acrylic acid) in DMSO-d_6 at 500 MHz frequency. The inset shows the magnified region of the ⟩C═O region.

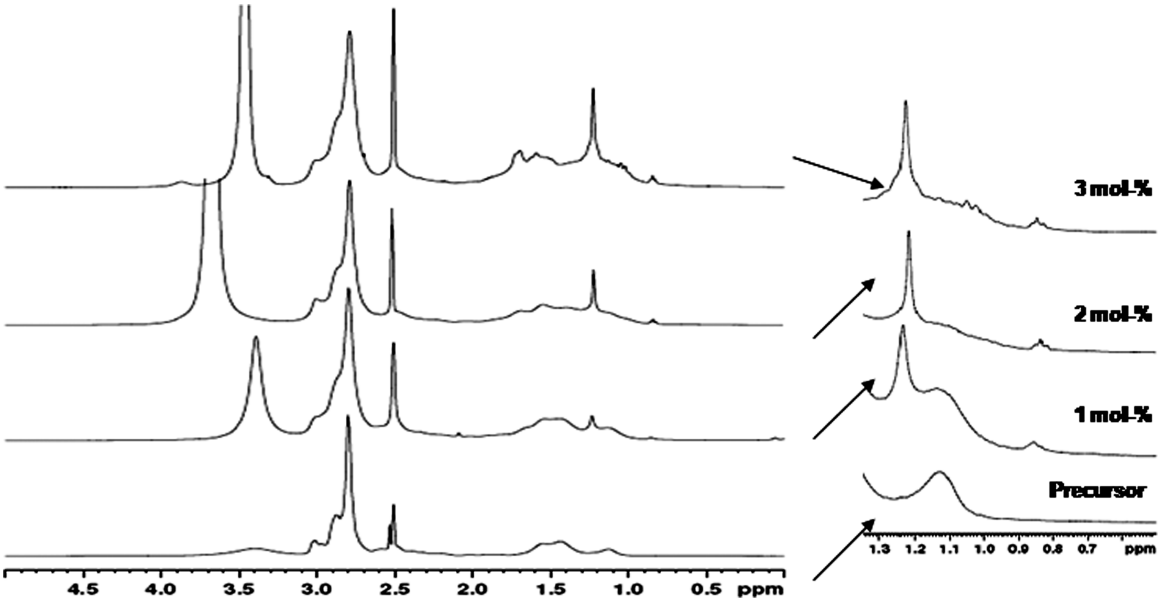

Figure 2. ^{1}H NMR spectra of precursor and hydrophobically modified poly(*N*,*N*′-dimethylacrylamide-*co*-acrylic acid), the latter having hydrophobe contents of 3-PDCA = 1, 2, and 3 mol %.

We show in Figure 2, the ^{1}H NMR spectra of hydrophobically modified poly(DMA-*co*-AA) with three different contents of 3-PDCA (1, 2, and 3 mol %) and compare them with the ^{1}H NMR spectrum of the precursor polymer.

The terminal $-CH_3$ attached to 3-PDCA group appeared at 0.82 ppm. Methylene ($-CH_2$) and methyne ($-CH$) protons of 3-PDCA and $-CH$ of polymer backbone appeared at 1.21 ppm. $-CH_2$ of the polymer backbone appeared at 1.53 ppm, and $-CH_3$ protons of $-N-CH_3$ group appear at 2.77 ppm (Figure 2). This is a clear evidence for the incorporation of 3-PDCA into the copolymer.

3.3. Rheology. *3.3.1. Concentration Dependence of Zero Shear Viscosity* (η_0). We show in Figure 3 the concentration dependence of η_0 for the precursor copolymer and for the hydrophobically modified copolymer containing 1, 2, and 3 mol % of 3-PDCA.

For the precursor copolymer the concentration range investigated in the present study is likely to be above the critical overlap concentration, C^*.[29] The data in Figure 3 show that the viscosity scaled with concentration as $\eta_0 \sim C_p^{0.7}$. The value of the exponent is in between that predicted by the so-called Fuoss law (0.5) and that of dilute solution (1.0), indicating that the copolymer is a flexible polyelectrolyte which most likely exists in a semidilute unentangled state in this concentration range.

For the hydrophobically modified polymers two regimes of η_0-C_p relations were observed. In the low-C_p regime the

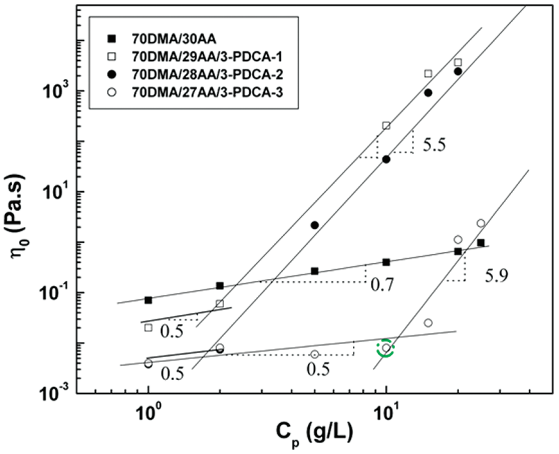

Figure 3. η_0 vs polymer concentration for precursor and hydrophobically modified poly(*N*,*N*′-dimethylacrylamide-*co*-acrylic acid) (3-PDCA = 1, 2, and 3 mol %).

viscosity scales with concentration as $\eta_0 \sim C_p^{0.5}$ following the Fuoss law. In this regime the viscosity of all hydrophobically modified copolymers was lower than that of the precursor copolymer at identical C_p. Further, the viscosity decreased with increase in hydrophobic content of the polymer. This lowering of viscosity of the hydrophobically modified copolymer relative to the precursor can be attributed to the shrinkage of coils due to intramolecular hydrophobic associations. Upon increase in concentration, the hydrophobically modified polymers showed sharp increase in viscosity above some critical aggregation concentration and surpassed the viscosity of the precursor. The concentration dependence was found to be $\eta_0 \sim C_p^x$, where the exponent was $x = 5.5-6.0$. Such a rapid increase in viscosity is due to the transformation of intramolecular hydrophobic associations (within isolated chains) into intermolecular hydrophobic associations (with overlapping chains) thereby forming aggregates, which eventually percolate to form self-supporting gels with further increase in concentration.

3.3.2. High Shear Rheology. Figure 4 shows viscosity vs shear rate data for various solutions of hydrophobically modified poly(*N*,*N*′-dimethylacrylamide-*co*-acrylic acid) containing 3 mol % of 3-PDCA at C_p ranging from 5 to 35 g/L. This data were obtained using the strain-controlled rheometer (ARES). The solution of $C_p = 5$ g/L showed a nearly Newtonian viscosity over the entire shear rate range $\dot{\gamma} = 10-1000\ s^{-1}$ studied here. Samples of higher concentrations, $C_p = 10$ g/L and above, also showed a Newtonian behavior at low shear rates, but this was followed by an abrupt shear thickening behavior of significant magnitude at critical shear rates ($\dot{\gamma}_{crit}$) which decreased with increasing C_p. The magnitude of shear thickening also decreased with increasing polymer concentration. These results are in qualitative agreement with those reported in earlier work.[23,24]

In the following, we present results obtained from stress-controlled experiments, specifically stress ramp and creep experiments, on one representative sample, 70DMA/27AA/3-PDCA-3; $C_p = 10$ g/L, which is demarcated in Figure 3. The C_p for this sample was close to the aggregation concentration, and as seen from Figure 4, an abrupt shear thickening effect was observed at a critical shear rate of $\sim 1000\ s^{-1}$. At lower shear rate the solution showed a viscosity $\eta = 0.01$ Pa s, which was nearly independent of shear rate. Small-amplitude oscillatory shear data on this solution showed a predominantly viscous behavior with no observable crossover of the shear moduli up to the highest frequency (100 rad/s) probed here.

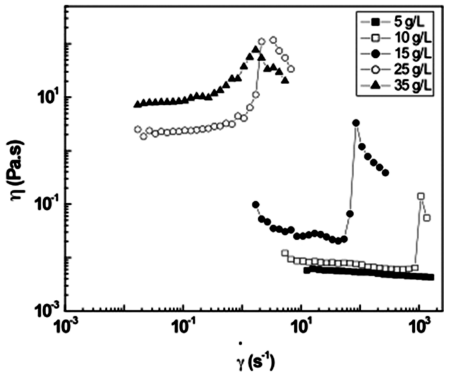

Figure 4. Plot of viscosity vs shear rate for 70DMA/27AA/3-PDCA-3 (C_p = 5, 10, 15, 25, and 35 g/L).

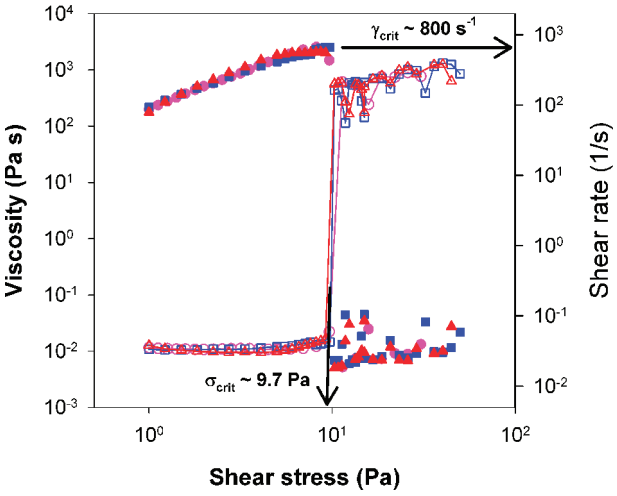

Figure 5. Stress-ramp experiment on the sample 70DMA/27AA/3-PDCA-3; $C_p = 10$ g/L.

Results of stress-ramp experiments are shown in Figure 5. Data are shown from three independent tests in which the shear stress was ramped up from 1 to 60 Pa. At low stresses the sample showed a Newtonian response with a viscosity of 0.01 Pa s (same as that obtained in the steady shear test performed on the strain-controlled rheometer, see Figure 4). Abrupt shear thickening was observed for this sample at a critical shear stress of $\sigma_{crit} \sim 10$ Pa and at a corresponding critical shear rate of $\dot{\gamma}_{crit} \sim 800\ s^{-1}$. Data obtained from more tests on this sample showed that σ_{crit} and $\dot{\gamma}_{crit}$ varied slightly between tests; for this particular sample, σ_{crit} varied between 8 and 10 Pa and $\dot{\gamma}_{crit}$ varied between 800 and 1100 s^{-1}. During all repeated tests the viscosity increased by as much as 5 orders of magnitude at the critical point, indicating the large magnitude of shear thickening effect. As expected, the shear rate dropped considerably upon shear thickening above σ_{crit} since only a small value of shear was required for the thickened sample to maintain the applied stress level. This minimized rupture or extrusion of the thickened sample from the geometry underlines the utility of performing stress ramp experiments.

To study the nature of the shear thickened sample further, we carried out creep experiments at various shear stresses below and above σ_{crit}. Figure 6 shows the evolution of creep compliance on application of various stresses. At stresses below the critical stress such as $\sigma = 5$ Pa the compliance grew continuously with time following the power law $J(t) \sim t^2$ at early time followed by a more gradual increase at long time. The early time response indicates inertia-controlled regime

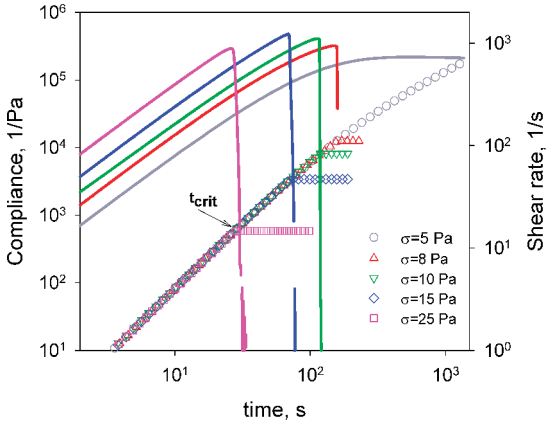

Figure 6. Evolution of creep compliance at various stress values for the sample 70DMA/27AA/3-PDCA-3; C_p = 10 g/L.

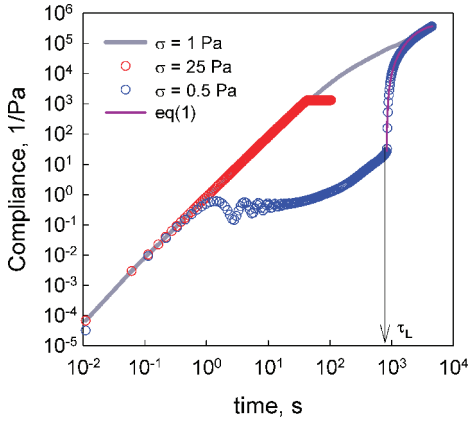

Figure 7. Compliance of the gel at 0.5 Pa after shear-induced gelation at 25 Pa. The recovery of compliance to the equilibrium liquids state starts at a critical time t_L and follows eq 1.

where the compliance approximately grows as $J(t) \simeq (b/2I)t^2$, b and I being respectively the geometrical parameter and inertia of the measuring system.[30] The continuous increase in compliance at long time reflects a typical viscous flow response of the solution. At stresses close to or above the critical stress, σ = 8, 10, 15, and 25 Pa, the compliance initially grew as $J(t) \sim t^2$ independent of the applied stress as expected but then abruptly reached plateau values, which decreased with increase in the applied stress. The occurrence of a compliance plateau is a clear indication of shear-induced gelation. Thus, the observed shear thickening effect is in fact a shear-induced gelation event, as also pointed out recently by Wang et al.[26] A decrease in the plateau value of compliance implies an increase in the modulus of the gel.

The time to gelation (t_{crit}) decreased with increase in applied stress. To understand this, we have also plotted in Figure 6 the temporal evolution of shear rate in each of the creep experiments. It can be seen that gelation was observed as soon as the shear rates reached values approximately equal to $\dot{\gamma}_{crit}$. The time to reach the critical shear rate was found to be inversely proportional to the shear stress, $t_{crit} \propto 1/\sigma$. This happens because in the initial inertia-controlled regime the strain grows as $\gamma \simeq (\sigma b/2I)t^2$ so that $t_{crit} \simeq (I\dot{\gamma}_{crit}/b\sigma)$. Data in Figure 6 unambiguously show that the shear-induced gelation event always occurs at a critical shear rate. Consequently, the creep experiments enable precise control on the formation of shear-induced gels of different moduli. We note here that such a control is not possible in a step shear experiment since the large imposed strain ruptures the soft gels upon formation.

The stability of shear-induced gels was studied by performing sequential creep experiments in which the gels were first formed by applying a stress $\sigma > \sigma_{crit}$ and then subjected to a lower stress $\sigma < \sigma_{crit}$. The compliance data from a typical experiment are shown in Figure 7. Here the sample was first subjected to a shear stress of 25 Pa until gelation occurred and then to a shear stress of 0.5 Pa for a long time. Upon lowering the stress to 0.5 Pa the compliance shows damped oscillations at short time ($t < t_{ringing}$) followed by a gradual increase at long time $t < t_{ringing} < \tau_L$. The damped oscillatory response, also called creep ringing, occurs because of the coupling between the elasticity of the gel and the inertia of the rheometer.[30] By fitting the creep ringing data to the Jeffery model, we may deduce the values of three material parameters: the gel modulus, relaxation time, and retardation time, which describe the viscoelasticity of the gel. For the 0.5 Pa creep data shown in Figure 7 these values are 2.5 Pa, 0.4 s, and 14.5 s, respectively.

Two interesting observations can be made from Figure 7. First, the compliance of the gel at σ = 0.5 Pa is *lower* than the compliance of the gel at σ = 25 Pa, implying that the gel formed at the higher stress of 25 Pa has a lower modulus (0.012 Pa) compared to the one that it transforms into (of modulus 2.5 Pa) upon lowering the stress to 0.5 Pa. Consequently, the stability of the gel formed at stresses $\sigma > \sigma_{crit}$ cannot be probed at lower stresses because the shear-induced gel itself transforms into a different state upon lowering the stress. In previous works the relaxation of shear-thickened solutions was studied by performing small-amplitude oscillatory shear measurements in a time sweep mode and measuring the decrease of dynamic moduli with time.[24] The storage modulus was observed to follow a stretched exponential relaxation. In the light of the results shown in Figure 7 it is evident that the relaxation event should not be viewed as the relaxation of a gel formed at the high shear conditions, but rather as the relaxation of a *different* gel that is formed when the shear-thickened sample is suddenly subjected to low-shear conditions.

The second interesting observation from Figure 7 is that there happens to be a critical "liquefaction" time τ_L at which the gel rapidly starts relaxing back to its equilibrium liquid state under quiescent conditions. The increase in compliance during the relaxation process can be described by

$$J(t) = J_L + J_1\left[1 - \exp\left(\frac{t-\tau_L}{\tau_g}\right)^{\alpha}\right] \qquad (1)$$

J_L is the compliance at τ_L, τ_g is a characteristic retardation time of the gel, and J_1 and α are constants. For the data shown in Figure 7 the variables J_L, J_1, τ_L, and τ_g have values of 28.3 Pa^{-1}, 4 × 10^5 Pa^{-1}, 836 s, and 2000 s, respectively. The value of α was observed to be 1.5, indicating a compressed exponential behavior for the liquefaction process. At long time the compliance of the sample asymptotically reached that of the equilibrium liquid state at $\sigma < \sigma_{crit}$.

The liquefaction (or gel to sol) transition was further investigated by subjecting the gel formed at a high stress $\sigma > \sigma_{crit}$ to different stress levels below the critical stress. Representative data are shown in Figure 8. In this experiment the solution was first subjected to a stress of 5 Pa, which was below the critical stress. Next, gelation was induced by shearing the solution at a stress of 10 Pa, which is close to the critical stress. In separate experiments the gel was then allowed to recover at different stresses of 1, 2, 3, 5, and 7 Pa, which are all below the critical stress. In each experiment

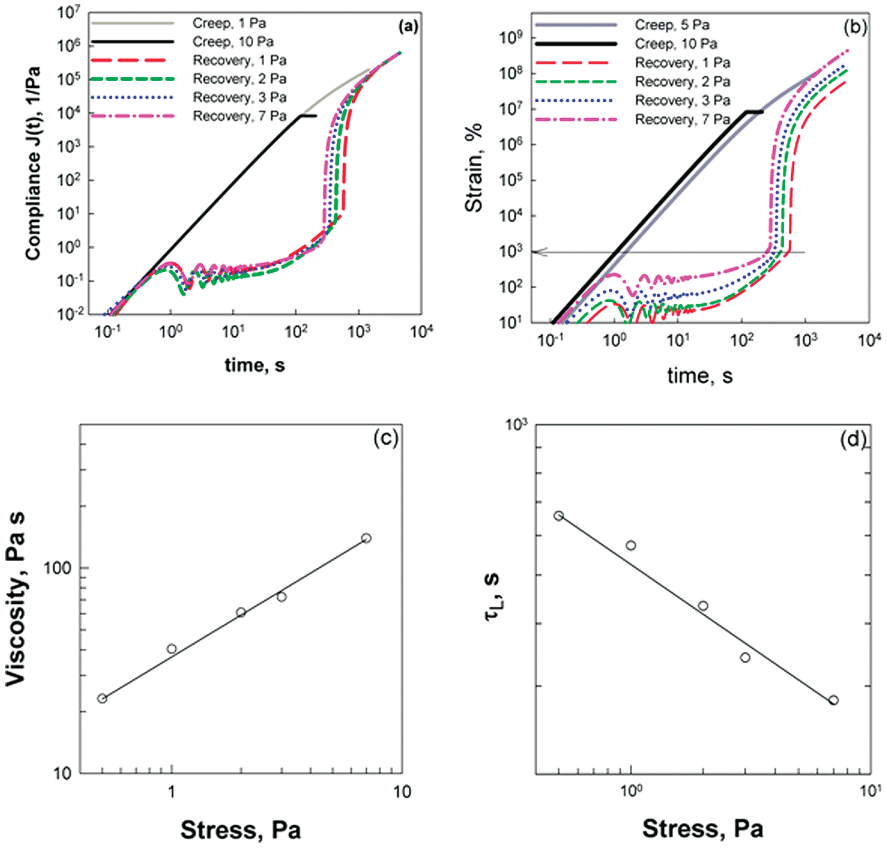

Figure 8. Gel to solution transition of a shear-induced gel at various stresses below the critical stress. The modulus of the gel is independent of stress (top left), but its viscosity shows a power law dependence on stress (bottom left). The liquefaction happens at a constant critical strain (top right), and the critical time for liquefaction decreases with stress (bottom right).

the sample was allowed to recover fully. It was assumed that recovery was complete when the compliance asymptotically reached the 5 Pa data. The next experiment was then performed on the same sample by first shearing it at 10 Pa and then allowing it to recover at the next value of stress.

The data in Figure 8a show that the short time compliance of the gel (damped oscillatory response) and hence the modulus of the gel formed at 1, 2, 3, 5, or 7 Pa are independent of the applied stress to within experimental error. However, the critical time (τ_L) at which liquefaction starts and the value of the compliance at that time (J_L) decreased with increase in stress. It was found that J_L varied inversely with the applied stress so that when the same data were plotted as strain versus time (Figure 8b), the liquefaction of the gel was found to start when a critical strain, independent of the probe stress, was reached. For the particular sample shown in Figure 8, the critical strain is 1000%. The liquefaction time τ_L showed a power law decrease with stress, $\tau_L \sim \sigma^{-0.33}$, as shown in Figure 8d. This can be explained as follows: The long time Newtonian creep response of the viscoelastic gel is given as $\gamma = t\sigma/\eta$ where G and η are respectively the modulus and viscosity of the gel. As mentioned earlier, the modulus G is independent of the applied stress. However, a careful inspection of the data in Figure 8b shows that the viscosity of the gel increased with the applied stress, $\eta \propto \sigma^{0.67}$, as shown in Figure 8c. Substitution of this in the equation for strain explains the observed power law for the stress dependence of the critical liquefaction time.

4. Discussion

As mentioned earlier, currently available transient network models for associating polymer solutions can predict, with reasonable accuracy, only *gradual* and relatively *mild* shear thickening phenomenon. Furthermore, these models are applicable for the case of high polymer concentration for which the average distance between associated clusters is less than the size of the chain. Consequently, the existing models cannot explain the abrupt and large extent of shear thickening (see Figure 5) observed for the polymer solutions in this work.

In order to gain some insights into the abrupt shear thickening phenomenon, we shall analyze the rheological data presented in the previous section for the sample 70DMA/27AA/3-PDCA-3; C_p = 10 g/L. Given that 3 mol % of the acrylic acid repeat units of this copolymer were modified with 3-PDCA units, the number of hydrophobes per chain is estimated to be approximately α = 124. In the quiescent state since the viscosity of this sample is much less than that of the precursor polymer, it is reasonable to expect that most of the hydrophobes are micellized within a single chain; i.e., they form intrachain associations. It has been suggested that hydrophobes containing linear alkyl chains show an aggregate number of 40 hydrophobes per micelle.[26] Assuming that this is an approximately correct representation for our polymer, we estimate that there are on an average three micelles per chain.

Figure 6 represents the first important result of this paper. It provides an unambiguous support for the argument that shear thickening occurs at a critical shear rate, which for the sample studied here was $\dot{\gamma}_{crit}$ = 800−1100 s^{-1}. This suggests that the onset of thickening requires a critical Weissenberg number $Wi_{crit} = \tau\dot{\gamma}_{crit}$, τ being a characteristic relaxation time of the viscous solution at low shear rates. From small-amplitude oscillatory measurements on this sample it appears that the relaxation time of the solution was less than 0.01 s. It is therefore possible that $Wi_{crit} \geq 1$. As the Weissenberg number reaches the critical value, chains that dissociate from the intrachain micelles by thermal fluctuations or are

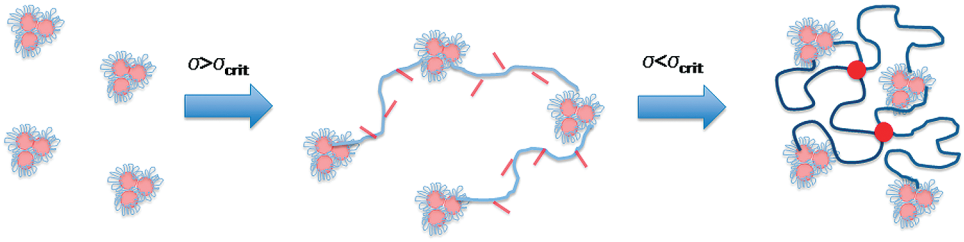

Figure 9. Schematic showing a mechanism for the formation of interchain associations upon cessation of flow. The initial solution at rest (leftmost) contains predominantly free chains that are in a collapsed conformation due to intramolecular associations (red circles). Upon application of stress $\sigma > \sigma_{crit}$ a few chains in the initial solution are stretched to large enough extents so that they form elastically active bridging chains. Percolation of such chains causes gelation, leading to the observed shear-thickening effect. However, a large number of hydrophobic groups (short red lines) on the stretched chains remain unassociated. Upon reduction of imposed stress $\sigma < \sigma_{crit}$ the gel relaxes, causing the bridging stretched chains to relax in an affine manner (bold lines) and attain a size that is *larger* than their equilibrium size because of lack of intrachain associations. The large coil size leads to chain overlap, thus enabling the formation of more interchain associations (dark red circle) between the free hydrophobes. Thus, the density of bridging chains increases, thereby leading to an increase in the modulus of the gel. Since the bridging chains are in a metastable conformation, they eventually reach their equilibrium collapsed conformations by loss of the interchain associations due to thermal fluctuations. This is seen as the relaxation event.

pulled out by the imposed shear would stretch out. The free hydrophobes on these chains would then have to quickly find other hydrophobes, and since the probability of finding such hydrophobes from other chains is finite in a semidilute solution, intrachain associations might form. These would act as transient cross-links that link bridging chains into a percolating network, resulting in gelation.

At this point it is important to look at the physics of coil-to-stretch transitions of single flexible polymer chains undergoing shear. In particular, it is worth noting that the results reported by Smith et al.[31] on fluorescent labeled lambda bacteriophage DNA in shear flow do not support the existence of a critical Weissenberg number for the coil to stretch transition. Rather, the time and ensemble average fractional extension of chains increases gradually with Weissenberg number. Observations of several chains at $Wi \gg 1$ showed that only a fraction of the chains are occasionally fully stretched by the flow. However, the frequency of fluctuations in chain extension increases with Weissenberg number. It is reasonable to assume that the high molecular weight hydrophobically modified polymers studied here follow qualitatively the observations made for DNA chains. This implies that the critical Weissenberg number observed for shear-induced gelation is likely to be related to a percolation effect in which a few chains stretch to sufficient extension to cause a percolated network of interconnected interchain clusters.

Indeed, the number density of elastically active chains estimated from the plateau compliance values, J_0, for the different stresses $\sigma > \sigma_{crit}$ shown in Figure 6 are much smaller than the limiting number of elastically active chains suggested by the chemical modification. The number density of elastically active chains at a given imposed stress can be calculated as $\nu = 1/(J_0 kT)$, while the theoretical limit of the number density of elastically active chains, assuming that all hydrophobes of a given chain are involved only in interchain associations, is given as $\nu_{max} = (\alpha - 1)C_p N_A/M_w$, N_A being the Avogadro number. Table 2 shows the fraction of elastically active chains created at the different imposed stresses shown in Figure 6. From these numbers it is clear that shear-induced gelation involves only a small fraction of the maximum available number of elastically active bridging chains. It is interesting to note that ν/ν_{max} increases with stress although gelation happens at nearly the same shear rate $\dot{\gamma} = \dot{\gamma}_{crit}$. This suggests that the fraction of chains that stretch and form elastically active strands seems to increase with the rate of increase of shear rate, which increases with the imposed stress. In other words, at any point of time during the experiment a higher value of imposed stress implies a higher shear rate and consequently a greater fraction of chains that get stretched to form a gel with a higher fraction of elastically active bridging chains.

Figure 4 shows that the magnitude of shear thickening and the critical shear rate for gelation decreased with increase in the concentration of the polymer. These observations can be attributed to the fact that at high polymer concentration there already exist a larger number of intermolecular hydrophobic associations even at near quiescent state so that imposition of shear causes a further small increase in the fraction of bridging chains. Also, since the zero shear viscosity of the samples is high (see Figure 3), the chains have longer relaxation times, and therefore, it is easier to stretch them. Hence, the critical shear rate required for further gelation decreases with C_p.

The above discussion suggests that theoretical models for abrupt shear thickening phenomenon must include the dynamics of shear-induced stretching of chains as well as percolation effects.

The second important result of this paper is shown in Figure 7. An intriguing feature of this data is that upon reduction of the imposed shear stress immediately after the shear-induced gelation event the modulus of the gel *increases* by several orders of magnitude. None of the existing models for shear thickening can explain this observation. If interpreted in terms of the fraction of elastically active chains, the value of ν/ν_{max} increases by as much as 3 orders of magnitude upon reduction in stress relative to the modulus of the shear induced gel formed at a high stress (see Table 2). However, ν/ν_{max} is still $\ll 1$. One possible explanation of this phenomenon is shown schematically in Figure 9. Upon imposition of a high stress $\sigma > \sigma_{crit}$ a few chains stretch to large enough extension so that a few hydrophobic groups on these chains find hydrophobic groups on other chains to form a gel, whereas a large number of hydrophobic groups on these stretched chains remain unassociated. Immediately upon reduction of stress to $\sigma < \sigma_{crit}$ the stretched chains undergo affine retraction, and since the hydrophobic groups are as yet unassociated, the chains attain a size that is *larger* than the equilibrium size of the coil which has intrachain associations. This causes the dangling groups to form new associations with those of the neighboring chains, thereby increasing the number density of bridging chains.

Many repeat experiments were also performed (data not shown) in which shear-induced gels were formed at different values of stresses $\sigma > \sigma_{crit}$ after which the stress was reduced to a fixed value $\sigma < \sigma_{crit}$. It was observed from these experiments that the compliance of the gel formed immediately upon reduction of stress was independent of the value of the high stress at which the gel was formed. This suggests that while the number of bridging chains increases with stress, a much larger number of hydrophobic groups on these stretched chains remain unassociated at the high stresses. A large fraction of these groups associate during retraction of the chains upon reduction of stress, thereby forming gels whose modulus is independent of the initial state of stress.

Similarly, the data shown in Figure 8 suggest that the compliance of the gel formed immediately upon reduction of stress is also independent of the value of stress $\sigma < \sigma_{crit}$.

Another interesting observation from Figure 7 is that there appears to be a critical time τ_L at which the gel starts to liquefy rapidly and ultimately reaches the original solution state. The liquefaction of the gel underlines its metastable nature. The mechanism suggested in Figure 9 relates the metastability to the existence of coils having size larger than the equilibrium size of the chains. Eventually, the interchain associations break by thermal fluctuations and/or the imposed probe stress, causing the coils to reach their equilibrium state. For $t_{ringing} < t < \tau_L$ the average compliance of the gel shows a gradual increase; indeed, the inverse of the slope of this part of the data gives the viscosity of the gel. From a molecular perspective the gel slowly creeps because of breakage of some of the interchain associations. Data in Figure 8 show that the viscosity of the gel increases with the applied stress $\sigma < \sigma_{crit}$. The small amount of thickening is possibly caused by shear-induced reformation of interchain associations. Eventually the gel seems to liquefy rapidly when the strain reaches some critical value. Higher imposed stress causes the gel to reach this value earlier so that τ_L decreases with imposed stress. A probable molecular interpretation could be that the tension in strongly held bridging chains reaches a critical point at the critical strain, causing rapid breakage of the interchain associations.

5. Conclusions

We have synthesized a high molecular weight hydrophobically modified copolymer and investigated the abrupt shear thickening properties of its solutions. By performing creep experiments on a stress-controlled rheometer, we have demonstrated several new attributes of the shear thickening phenomenon and the subsequent relaxation process, which have hitherto not been reported. In particular, we have shown that shear-induced thickening is a gelation process that happens at a critical shear rate and that it is possible to trap the gel in different metastable states by imposing different stresses above the critical stress. Furthermore, we have shown that the linear rheological properties of such shear-induced gels cannot be studied by dropping the probe stress values to small levels because the process of doing so itself changes the state of the gel. Remarkably, reducing the stress after gelation in fact results in the formation of stiffer gels. The modulus of the gels so formed is, to a large extent, independent of the stress level at which gelation happened as also the stress level at which recovery was probed after gelation. We have suggested that shear-thickened gels are formed when only a few chains are stretched sufficiently at the critical shear rate to enable interchain associations of a few hydrophobic groups on these chains. Percolation of these stretched bridging chains causes gelation, but many hydrophobic groups on them remain unassociated. Further stiffening of the shear-thickened gels upon reduction of stress occurs when the bridging chains retract and attain coil size larger than the equilibrium size so that the unassociated hydrophobic groups form further interchain associations. Finally, we have shown that liquefaction of the gels occurs at a critical time, when a critical strain is reached. The present models to explain the shear-thickening phenomenon do not explain any of these observations satisfactorily. We suggest that further experimental investigations in stress-controlled rheometry as well as renewed modeling efforts are necessary to understand the experimental observations presented here.

Acknowledgment. A. S. Shedge is grateful to CSIR, New Delhi, for the Senior Research Fellowship (SRF). The financial support from DST, New Delhi, is also gratefully acknowledged.

References and Notes

(1) Broze, G.; Jerome, R.; Teyssie, P.; Marco, C. *Macromolecules* **1983**, *16*, 996–1000.
(2) Ma, S. X.; Cooper, S. L. *Macromolecules* **2001**, *34*, 3294–3301.
(3) Egmond von, J. W. *Curr. Opin. Colloid Interface Sci.* **1998**, *3*, 385–390.
(4) Barnes, H. A. *J. Rheol.* **1989**, *33*, 329–366.
(5) Wagner, N. J.; Brady, J. F. *Phys. Today* **2009**, *10*, 27–32.
(6) Tanaka, F.; Edwards, S. F. *J. Non-Newtonian Fluid Mech.* **1992**, *43*, 247–271.
(7) Tanaka, F.; Edwards, S. F. *J. Non-Newtonian Fluid Mech.* **1992**, *43*, 273–288.
(8) Tanaka, F.; Edwards, S. F. *J. Non-Newtonian Fluid Mech.* **1992**, *43*, 289–309.
(9) Tanaka, F.; Edwards, S. F. *Macromolecules* **1992**, *25*, 1516–1523.
(10) Green, M. S.; Tobolsky, A. V. *J. Chem. Phys.* **1946**, *14*, 80–89.
(11) Witten, T. A.; Cohen, M. H. *Macromolecules* **1985**, *18*, 1915–1918.
(12) Ballard, M. J.; Buscall, R.; Waite, F. A. *Polymer* **1988**, *29*, 1287–1293.
(13) Wang, S. Q. *Macromolecules* **1992**, *25*, 7003–7010.
(14) Marrucci, G.; Bhargava, S.; Cooper, S. L. *Macromolecules* **1993**, *26*, 6483–6488.
(15) Vrahopoulou, E. P.; McHugh, A. J. *J. Rheol.* **1987**, *31*, 371–384.
(16) Vandenbrule, B. H. A. A.; Hoogerbrugge, P. J. *J. Non-Newtonian Fluid Mech.* **1995**, *60*, 303–334.
(17) Vaccaro, A.; Marrucci, G. *J. Non-Newtonian Fluid Mech.* **2000**, *92*, 261–273.
(18) Ahn, K. H.; Osaki, K. *J. Non-Newtonian Fluid Mech.* **1995**, *56*, 267–288.
(19) Lele, A. K.; Mashelkar, R. A. *J. Non-Newtonian Fluid Mech.* **1998**, *75*, 99–115.
(20) Tripathi, A.; Tam, K. C.; McKinley, G. H. *Macromolecules* **2006**, *39*, 1981–1999.
(21) Peiffer, D. G.; Lundberg, R. D.; Duvdevani, A. *Polymer* **1986**, *27*, 1453–1462.
(22) Dupuis, D.; Lewandowski, F. Y.; Steiert, P.; Wolff, C. *J. Non-Newtonian Fluid Mech.* **1994**, *54*, 11–32.
(23) Bokias, G.; Hourdet, D.; Iliopoulos, I. *Macromolecules* **2000**, *33*, 2929–2935.
(24) Cadix, A.; Chasseneuix, C.; Lafuma, F.; Lequeux, F. *Macromolecules* **2005**, *38*, 527–538.
(25) Rubinstein, M.; Semenov, A. *Macromolecules* **2001**, *34*, 1058–1068.
(26) Wang, J.; Benyahiya, L.; Chassenieux, C.; Tassin, J.-F.; Nicolai, T. *Polymer* **2010**, *51*, 1964–1971.
(27) Shedge, A. S.; Lele, A. K.; Wadgaonkar, P. P.; Hourdet, D.; Perrin, P.; Chassenieux, C.; Badiger, M. V. *Macromol. Chem. Phys.* **2005**, *206*, 464–472.
(28) Tanford, C. *Hydrophobic Effect: Formation of Micelles and Biological Membranes*, 2nd ed.; John Wiley and Sons Inc.: New York, 1980.
(29) The overlap concentration for aqueous solutions of nonionic polyacrylamide of molecular weight similar to that of the precursor polymer (~1200 kg/mol) is known to be about 0.8 g/L (Grigorescu, G.; Kulicke, W.-M. *Adv. Polym. Sci.* **2000**, *152*, 1–39). Therefore, it is likely that the C* for precursor polymer is of the same order or magnitude.
(30) Ewoldt, R. H.; McKinley, G. H. *Rheol. Bull.* **2007**, *76*, 4–24.
(31) Smith, D. E.; Babcock, H. P.; Chu, S. *Science* **1999**, *283*, 1724–1727.